DINAME 2023 - Proceedings of the XIX International Symposium on Dynamic Problems of Mechanics,
A.S. De Paula, A.T. Fabro and M.R. Machado (Editors), ABCM.
Pirenópolis, Go, Brazil, February 26th to March 3rd, 2023

Vibration attenuation and chaos in periodic lattices with bi-stable resonators

André Brandão[1], Aline Souza de Paula[1], and Adriano Fabro[1]

[1]Department of Mechanical Engineering, University of Brasília, Brasília-DF, Brazil.

Abstract: The interest for the study of metamaterials and metastructures has been rapidly increasing in the scientific community. A number of different approaches for the configuration of such systems have already shown to produce unique and potentially useful dynamic behaviour, such as broadband vibration attenuation. Locally resonant metamaterials are of special interest in this domain because of their versatility in creating wide bandgaps for wave propagation while being relatively simple in terms of analysis and mechanical design. Most remarkably, nonlinear metamaterials have been attracting increasing research interest due to their interesting enhanced vibration attenuation capabilities. This work presents an investigation of a nonlinear periodic metamaterial attached to a main structure with aiming at understanding the mechanisms responsible for such enhanced attenuation characteristics. An analysis of the frequency response content ultimately reveals that chaotic behavior arising from an arrangement of bistable resonators can produce broadband vibration attenuation on a simple 1-D periodic lattice system.

Keywords: nonlinear metastructures, vibration attenuation, chaos, bi-stable resonators

INTRODUCTION

In the last decades, metamaterials have been widely explored for several engineering applications, including vibration control [1, 2, 3]. The effects arising from these systems' periodicity and local resonance characteristics can be explored for enhancing the structural dynamics and broadband attenuation [4].

In recent years, a significant growth in the research of nonlinear periodic structures has been observed. Most of the literature focus on the enhanced bandgap performance of such structures or on the characterization of nonlinear phenomena and transition between periodic and chaotic behaviors.

Recent works by Xia et al. [5, 6] describe a system consisting of an elastic beam with identical bi-stable local resonators with an investigation of the effects of such nonlinearity in the system's frequency response for different excitation levels. The system exhibits rich dynamic behavior with linear intrawell, nonlinear intrawell and interwell behavior. For higher excitation levels. the system reaches chaotic behavior which ends up improving considerably the vibration attenuation performance outside the bandgaps. In the work, both harmonic balance method and time-domain integration are used to obtain the results.

Sheng et al. presented in 2021 [7] numerical and experimental results of a beam with nonlinear resonator attachments. The nonlinear resonator unit cell consists in a complex arrangement of a Duffing oscillator, a flexural resonator and a vibro-impact resonator. The results show significant vibration attenuation enhancement, specially in the conditions resulting in chaotic behavior. Different variations in the system's parameters are studied to assess the impact on the final attenuation performance. Another interesting conclusion is the increasing attenuation rate with increased excitation amplitude, which is a direct consequence of the introduced nonlinearities.

This work presents an arrangement of a 1-D periodic lattice with bi-stable Duffing resonator attachments, showing the effects of excitation magnitude on vibration attenuation. An investigation of the vibration attenuation mechanisms considering frequency-domain approach is also developed. This simple arrangement allows us to thoroughly investigate and understand the mechanisms responsible for vibration attenuation in the nonlinear system, especially when chaotic behavior is observed.

SYSTEM DESCRIPTION

The schematic drawing shown in Figure 1 depicts the N_0 DOF 1-D periodic chain with nonlinear resonators periodically attached considered in this study. The mass of each resonator is represented by $m_n = m_0$, $n = 1..N_1$, being m_0 a reference mass value. The linear elastic elements that connects the chain elements are identical, with stiffness k_0, and it is also considered a linear viscous damping c_0 between each element.

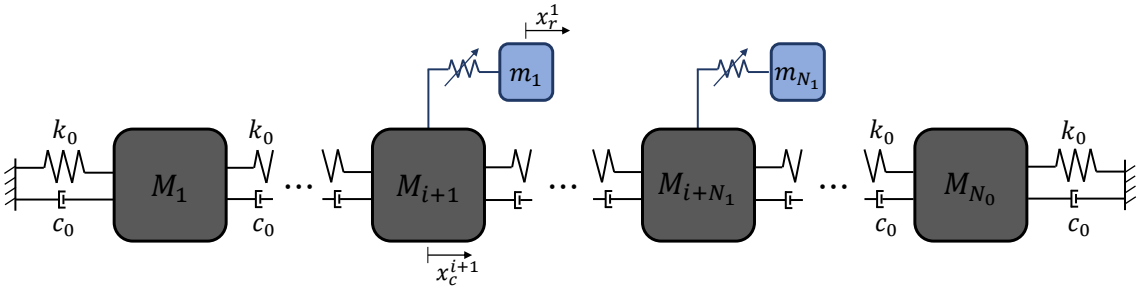

Figure 1: 1-D chain arrangement used for the simulations in this chapter.

The system's equation of motion in homogeneous form can be described as

$$\mathbf{[M]}\ddot{\mathbf{x}} + \mathbf{[C]}\dot{\mathbf{x}} + \mathbf{[K]}\mathbf{x} + \mathbf{f}_{nl}(\mathbf{x}) = 0 \qquad ; \qquad \mathbf{x} = \begin{Bmatrix} \mathbf{x}_c \\ \mathbf{x}_r \end{Bmatrix}, \tag{1}$$

in which **[M]**, **[C]** and **[K]** are the system's linear mass, damping and stiffness matrices, respectively, $\mathbf{f}_{nl}(\mathbf{x})$ is a vector representing the nonlinear effects and $\mathbf{x}_c$ and $\mathbf{x}_r$ are the displacement vectors for the chain and resonators, respectively.

The behavior of the nonlinear resonators, composed by a lumped mass and a nonlinear elastic element, is described by the Duffing equation [8]. This type of oscillator is one of the most used in studies of nonlinear mechanical structures due to its mathematical simplicity and richness in dynamic behavior. Another advantage of this oscillator is that it can be reproduced in real experimental setups, as shown in recent works [6]. Thus, the equation of motion of each resonator is described by

$$m_n \ddot{x}_r^n + \delta \dot{\tilde{x}}_n + \beta \tilde{x}_n + \alpha \tilde{x}_n^3 = 0 \tag{2}$$

where $\tilde{x}_n = x_r^n - x_c^{i+n}$ is the relative displacement between each resonator and the chain element to which it is attached, with x_r^n and x_c^{i+n} being individual components of the vectors $\mathbf{x}_r$ and $\mathbf{x}_c$. Note that the terms related to the coefficients m_n, δ and β are linear, and can be included in the linear matrices described in Equation 1. The only nonlinear term in Equation 2 is $\alpha \tilde{x}_n^3$, which is included in the nonlinear force vector $\mathbf{f}_{nl}(\mathbf{x})$.

The restoring force of the conservative system is given by $F_r(x) = -\beta x - \alpha x^3$. Considering the special situation where $\beta < 0$ and $\alpha > 0$, the equation describes a bi-stable oscillator, which is the case explored in this study. From the positive non-zero root of the restoring force expression, we obtain the value of the stable equilibrium position $x_0 = \sqrt{\frac{-\beta}{\alpha}}$.

By integrating the restoring force expression it's possible to obtain an expression for the oscillator's potential energy $U_p(x) = \frac{1}{2}\beta x^2 + \frac{1}{4}\alpha x^4$. As a result, the oscillator has in fact 3 equilibrium conditions, being two of them stable at $x = x_0$ and $x = -x_0$ - also referred to as potential wells - and the third one an unstable equilibrium condition at $x = 0$.

Further exploring the restoring force expression, it is possible to calculate its derivative to obtain the value of the local linearized stiffness $k_{lin}(x_0)$ of the Duffing oscillator around its stable equilibrium position as

$$k_{lin}(x_0) = -\frac{dF_r}{dx}\bigg|_{x_0=\sqrt{\frac{-\beta}{\alpha}}} = (\beta + 3\alpha x^2)\big|_{x_0=\sqrt{\frac{-\beta}{\alpha}}} = -2\beta. \tag{3}$$

The linearized natural frequency of the resonators is defined in terms of the reference mass, m_0, as $\omega_0 = \sqrt{\frac{k_{lin}(x_0)}{m_0}}$, which enables one to obtain the Duffing equation parameters in terms of physical quantities as $\beta = -\frac{\omega_0^2 m_0}{2}$ and $\alpha = -\frac{\beta}{x_0^2}$. Thus, it is possible to evaluate the direct comparison with an analogous purely linear resonator of stiffness $k = -2\beta$.

NUMERICAL SOLUTION

To obtain the Frequency Response plots, a hybrid numerical procedure was considered, combining the Harmonic Balance Method (HBM) [9], used in the case of periodic response, and a direct-integration 4$^{\text{th}}$ order Runge-Kutta Method (RK4) for nonperiodic behavior. Additionally, to determine the stability of the periodic solution obtained by using HBM, Floquet Multipliers [10] were calculated. This section presents the HBM, Floquet Multipluers calculation and how the procedure is carried out.

Harmonic Balance Method

The Harmonic Balance Method (HBM) was first proposed and described in 1968 by Bailey in his PhD thesis [11] as a technique for finding steady-state periodic solutions for nonlinear circuits networks. The method proposes a periodic solution for nonlinear differential equations in the form of its Fourier Series. By the formulation of an error function, as optimization method is applied to find the Fourier coefficients by minimizing the error function.

Detroux et al. [9] present in deep detail a Harmonic Balance framework for Bifurcation Analysis in Nonlinear Mechanical Systems which is quite adequate for the purposes of this thesis. The proposed procedure uses an Alternating Frequency/Time-Domain (AFT) technique to compute the non-linear forces' harmonic components and build the Harmonic Balance problem. This procedure is the on used in this thesis, and is described in further detail in the remainder of this chapter.

The construction of the Harmonic Balance Method starts with the definition of the n-DoF system's equations of motion in the time-domain as

$$\mathbf{M}\ddot{\mathbf{x}} + \mathbf{C}\dot{\mathbf{x}} + \mathbf{K}\mathbf{x} = \mathbf{f}_{ext}(\omega, t) - \mathbf{f}_{nl}(\mathbf{x}, \dot{\mathbf{x}}) = \mathbf{f}(\mathbf{x}, \dot{\mathbf{x}}, \omega, t), \tag{4}$$

in which all non-linear effects are considered as the separate force component $\mathbf{f}_{nl}(\mathbf{x}, \dot{\mathbf{x}})$, the external excitation forces are represented by $\mathbf{f}_{ext}(\omega, t)$, $\mathbf{x}$ and $\dot{\mathbf{x}}$ are the state variables vectors and $\mathbf{M}$, $\mathbf{C}$ and $\mathbf{K}$ stand for the system's mass, damping and stiffness $n \times n$ matrices.

The time dependent elements in Equation 4 can then be approximated by the their Fourier series truncated at N_H:

$$\mathbf{x}(t) = \mathbf{c}_0^x + \sum_{k=1}^{N_H} \left[\mathbf{s}_k^x \sin\left(\frac{k\omega t}{\nu}\right) + \mathbf{c}_k^x \cos\left(\frac{k\omega t}{\nu}\right) \right] \tag{5}$$

$$\mathbf{f}(t) = \mathbf{c}_0^f + \sum_{k=1}^{N_H} \left[\mathbf{s}_k^f \sin\left(\frac{k\omega t}{\nu}\right) + \mathbf{c}_k^f \cos\left(\frac{k\omega t}{\nu}\right) \right] \tag{6}$$

where the vectors denoted by $\mathbf{c}_k$ and $\mathbf{s}_k$ contain the Fourier coefficients of the k-th harmonic for all n DoFs of the system.

Substituting the expressions of Equations 6 and 5 in Equation 4 yield the fundamental equation that defines the Harmonic Balance Method problem

$$\mathbf{h}(\mathbf{z}, \omega) \equiv \mathbf{A}(\omega)\mathbf{z} - \mathbf{b}(\mathbf{z}, \omega) = 0, \tag{7}$$

where $\mathbf{A}$ is the $(2N_H + 1)n \times (2N_H + 1)n$ matrix containing the information of the system's linear dynamics, whereas $\mathbf{b}$ is the vector containing the Fourier coefficients of both external and nonlinear forces combined and $\mathbf{z}$ is the vector containing the Fourier coefficients of the periodic solution.

The Harmonic Balance Method is then reduced to the optimization problem of finding the $\mathbf{z}$ coefficients that leads to $\mathbf{h}(\mathbf{z}, \omega) = 0$. It becomes clear that the choice of ω and ν, which ultimately define the frequency components considered in the search for a periodic solution, are also of great importance to the complete definition of the problem. To find the roots of Equation 7, however, since $\mathbf{b}$ depends on $\mathbf{z}$, an iterative process is required. In this work the modified Powell's Method available inthe Python-based SciPy Optimization library was used.

Floquet Multipliers

There are different methods for evaluating the stability of a system's behavior. When the interest is to determine if a specific periodic solution is stable, calculating the Floquet Multipliers associated with this solution's orbit can be the easiest alternative. First introduced by G. Floquet in 1883 [12] as a part of the study on differential equations with periodic coefficients, known as Floquet Theory, the Floquet Multipliers are a mathematical quantity that can reveal the asymptotic behavior of a given periodic solution of a known autonomous system.

As thoroughly described by [13] and [10], if we assume a certain nonlinear system defined by

$$x'(t) = f(x), \tag{8}$$

we can suppose that $y(t)$ is a periodic solution of Eq. 8, and $T > 0$ is the period of y. The behavior of solutions of this same equation with initial values close to the periodic orbit formed by $y(t)$ is determined by the *monodromy matrix* $\mathbf{M}$ defined as

$$\mathbf{M} = \left. \frac{\partial \phi_T(x_0)}{\partial x_0} \right|_{x_0 = y(0)}, \tag{9}$$

where $\phi_t(x_0)$ denote the solution of Eq. 8 at time t and starting from x_0 at time $t = 0$.

The eigenvalues $\lambda \neq 0$ of the monodromy matrix $\mathbf{M}$ are called *Floquet Multipliers*. There will always be at least one eigenvalue $\lambda = 1$, called the *trivial Floquet Multiplier*, with associated eigenvector $\mathbf{u}_0 = f'(y(0))$. If all non trivial Floquet Multipliers are found to fall within the complex unit circle, the periodic solution y is stable, and exponentially attracting to any other orbits close to ϕ_t. If any of the Floquet Multipliers are outside the complex unit circle, this solution is unstable.

The monodromy matrix can then be computed as the solution at time T of the variational equation

$$\frac{d\mathbf{M}(t)}{dt} = \left. \frac{\partial f(x)}{\partial x} \right|_{x=y(t)} \mathbf{M}(t) \quad , \quad \mathbf{M}(0) = I. \tag{10}$$

In this work, the solution to Eq. 10 was determined with a direct integration approach using 4th order Runge-Kutta method.

Numerical methods evaluation

Figure 2 shows the Frequency Response plots obtained by both HBM and direct integration procedures. The points indicated as Flagged (black points) correspond to situations where periodic solution could not be found, and the points marked as Unstable (red x) are periodic solution with at least one Floquet Multiplier greater than 1, therefore, correspond to unstable orbits.

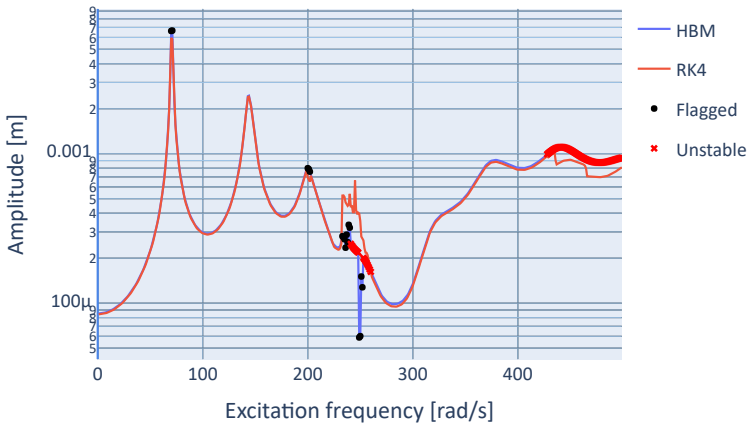

Figure 2: Frequency Response obtained with both HBM and direct integration. Periodic resonators and 4000 N excitation amplitude.

The Frequency Response plots shown henceforth were obtained using HBM as a standard. The direct integration method - Runge-Kutta 4th order - is only applied when the HBM is not able to find a valid periodic solution or if the solution found is shown to be unstable.

RESULTS

In all simulations a 20 DOF chain is considered, $N_0 = 20$, with identical mass elements, $M_n = 5$ kg, and linear stiffness coefficient of $k_0 = \frac{80}{d} kN/m$, where d is the distance between chain elements, fixed at $d = 0.05m$. A linear viscous damping is also considered between each two consecutive elements of the chain, being $c_0 = 2 \times 10^{-4} k_0$. Concerning the resonators, the reference natural frequency is fixed at $\omega_0 = 250$ rad/s and the dissipative term of the Duffing Equation is $\delta = -8 \times 10^{-4} \beta$. Is is considered 10 resonators, $N_1 = 10$, positioned at $i+1$, being the first resonator attached at $i+1 = 6$, each one with mass of $m_n = m_0 = 2.5kg$.

At first identical resonators are of concern and a harmonic excitation is applied to the leftmost element of the chain. Frequency response for different excitation amplitudes are shown in Figure 3 in terms of the RMS displacement of the

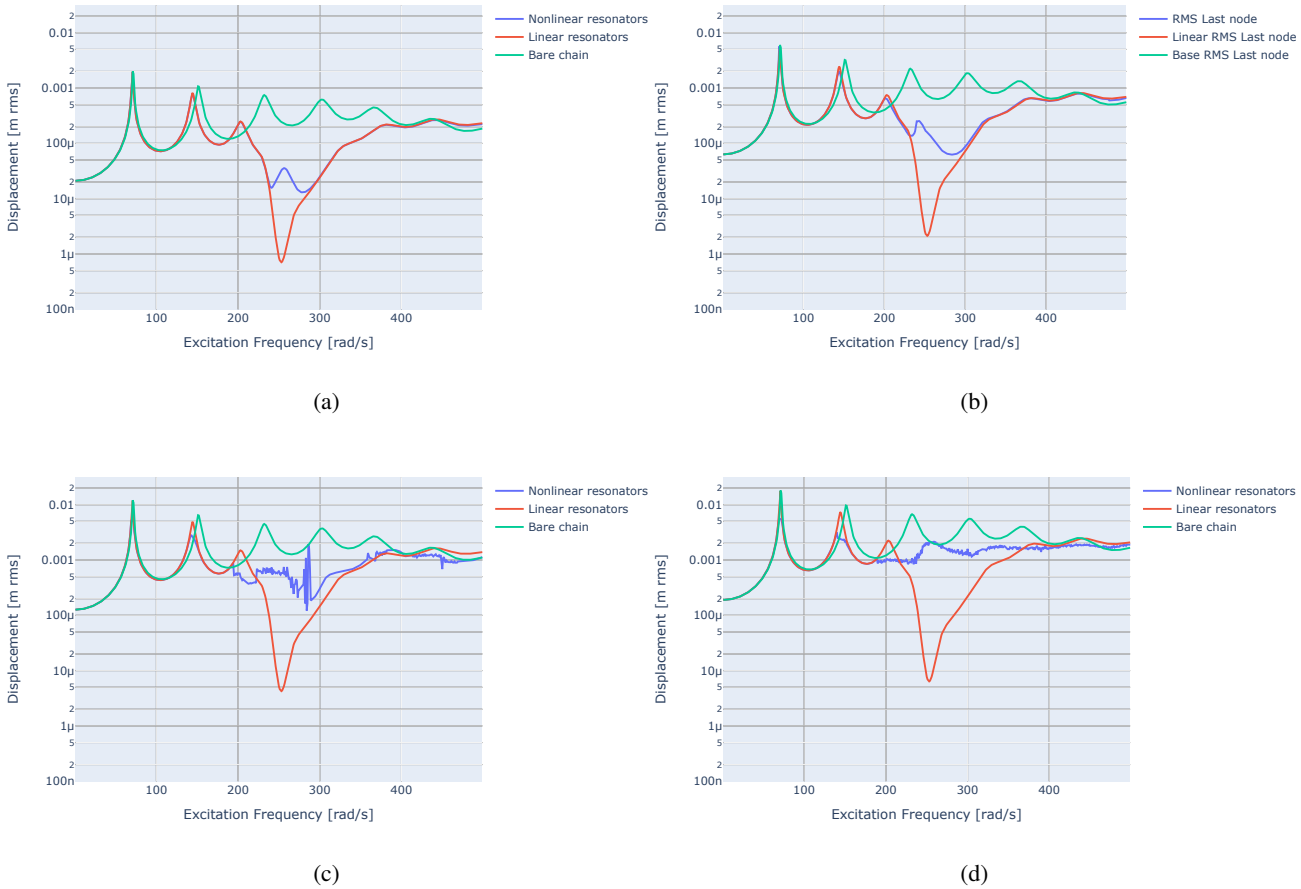

Figure 3: Frequency Response plots comparing the system's response for different excitation amplitudes: (a) 1000 N, (b) 3000 N, (c) 6000 N and (d) 9000 N.

rightmost element, opposite to the point where the excitation is applied. As excitation amplitude increases, the effect of the resonators' nonlinearities become more pronounced. Furthermore, as these nonlinear effects manifest themselves with greater strength, the chain response tends to exhibit a flat profile, with neutralisation of all natural frequencies, except for the first one.

It is important to notice that, although the excitation applied is purely harmonic, the nonlinear system may exhibit multi-harmonic or even broadband response. This is essential for the full comprehension of the underlying phenomena responsible for the vibration attenuation effects. The Bifurcation Diagrams at Figure 4 indicate chaotic behavior for some of the frequency bands with vibration attenuation. These diagrams consider the displacement of the last chain element.

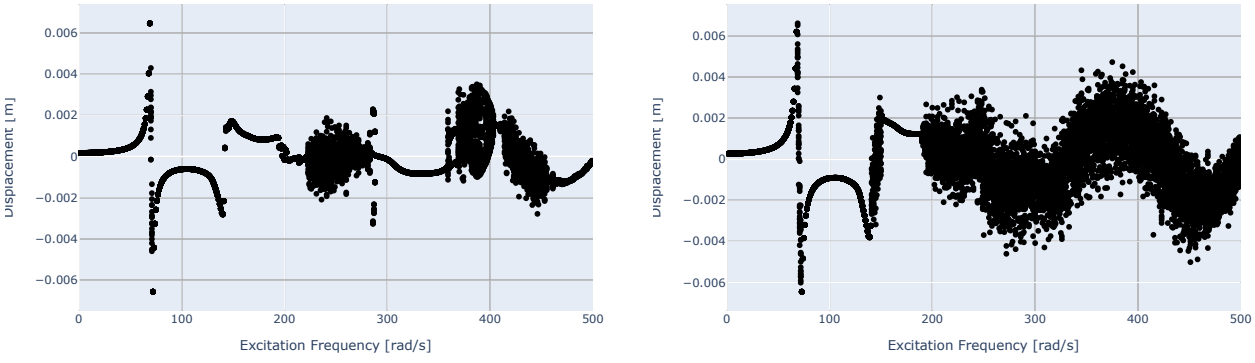

Figure 4: Bifurcation Diagrams for different excitation amplitudes: (a) 6000 N, (b) 9000 N.

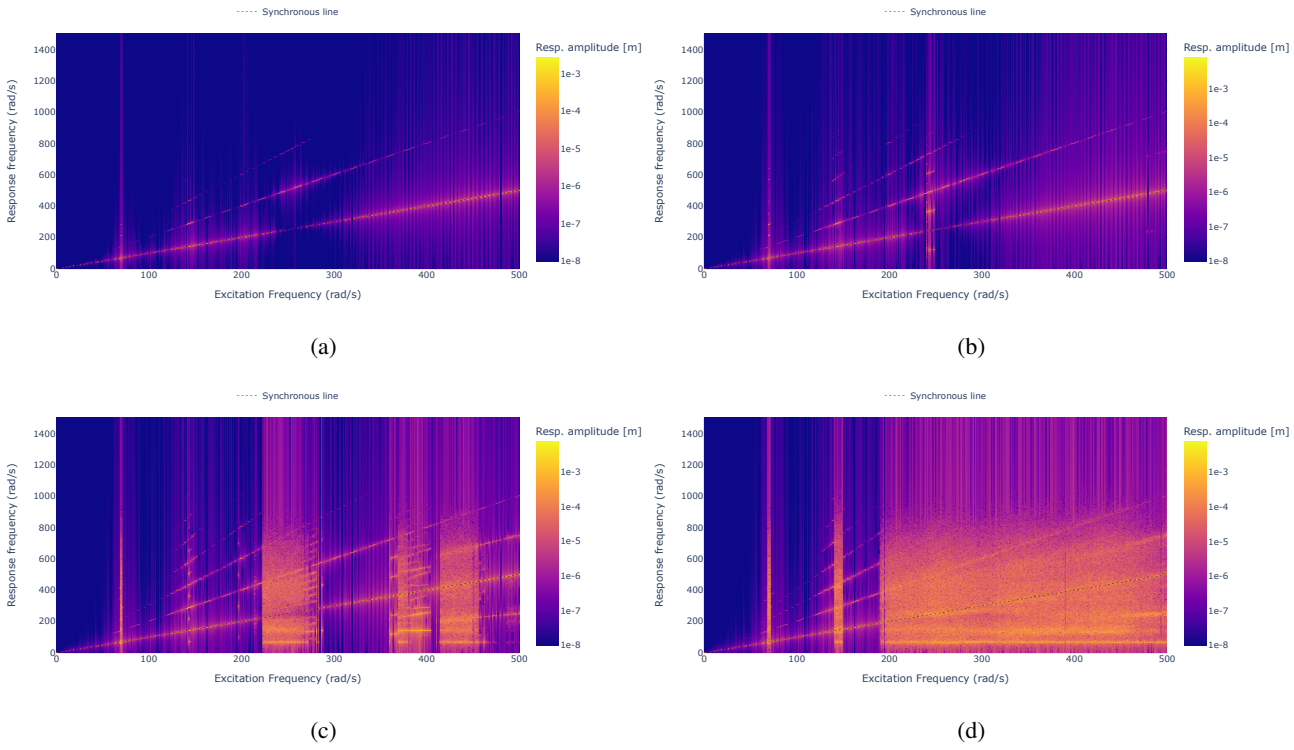

Figure 5: Frequency Response heatmap of the system for different excitation amplitudes: (a) 1000 N, (b) 3000 N, (c) 6000 N and (d) 9000 N.

To better understand the underlying phenomena occurring on the system, especially at the chaotic behavior, we can analyze the frequency content of the system's response. For that, the system's steady state response was considered and the Direct Fourier Transform (DFT) was calculated for each excitation frequency condition. The heatmaps presented in Figure 5 show the evolution of the frequency content in the response (Y axis) as a function of the excitation frequency (X axis). Some numerical noise can be observed, especially on the inter-harmonic spaces of periodic behavior, due to effects intrinsic to DFT calculation and which are amplified by the log-scale used.

Figure 5 shows a richer frequency distribution of the system's response as the excitation amplitude increases. For these plots, the response was obtained using the direct integration method for all cases. The spectral heatmaps make clear that different patterns of dynamic behavior emerge for different excitation conditions. In some conditions multi-harmonic periodic behavior appears to dominate the system's response. In other frequency regions, seemingly chaotic broadband response becomes present, where the first natural frequencies of the base chain, located between 70 Hz and 140 Hz, seem to be constantly excited.

To investigate the interaction mechanisms in each of these frequency regions with different behavior patterns, the amplification and phase difference between base structure and resonators are investigated. As described by Brandão et al. in [14], we can evaluate the interaction between resonators and base structure using the spatial average of the amplification

$$A_{\text{avg}} = \frac{1}{N_1} \sum_{n=1}^{N_1} A_i, \tag{11}$$

and phase difference

$$\phi_{\text{avg}} = \frac{1}{N_1} \sum_{n=1}^{N_1} \phi_i, \tag{12}$$

between the N_1 resonators and main structure. To apply this concept to the system's response, $X^i_{\text{res}}/X^i_{\text{chain}} = A_i e^{j\phi_i}$, where X^i_{res} and X^i_{chain} are the complex amplitudes of each frequency component corresponding to the i^{th} resonator and the chain node to which it is attached. These spatial averages are shown for different excitation amplitudes in the heatmaps of Figure 6 for 1 kN, Figure 7 for 6 kN and Figure 8 for 9 kN.

The amplification patterns observed in Figures 6 to 8 show that when periodic motion is dominant the attenuation mechanisms are similar to those observed in linear systems, in which the phase relation between resonators and base

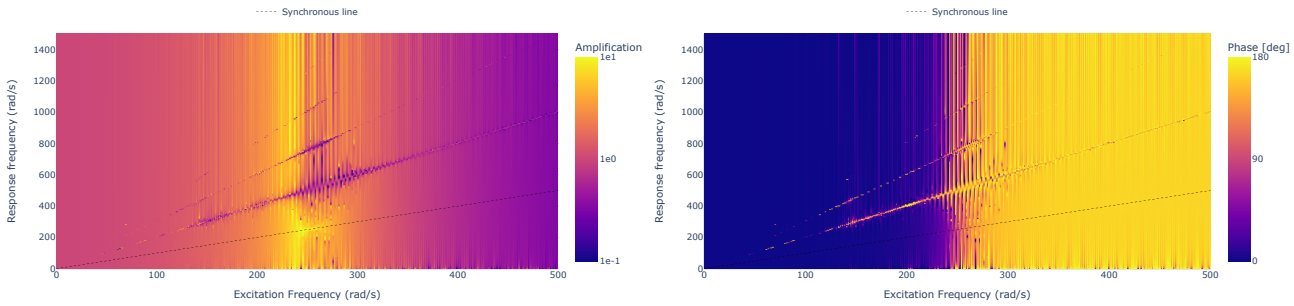

(a) (b)

Figure 6: Spatially averaged amplification (a) and relative phase (b) between base chain and resonators for excitation amplitude of 1000 N.

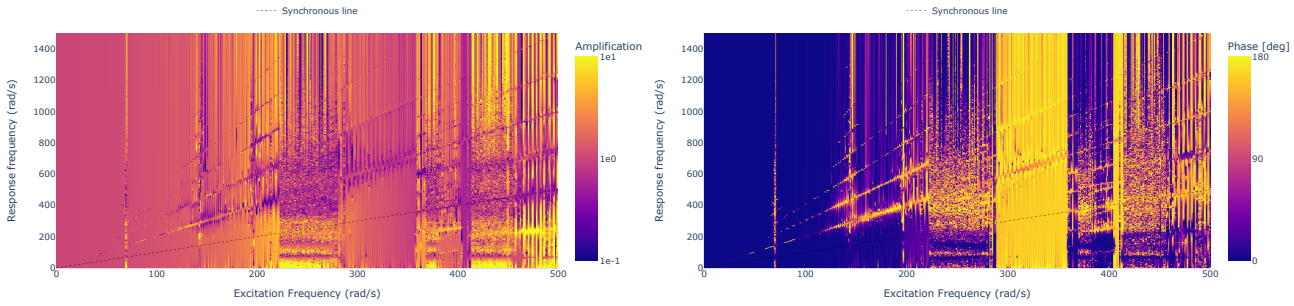

(a) (b)

Figure 7: Spatially averaged amplification (a) and relative phase (b) between base chain and resonators for excitation amplitude of 6000 N.

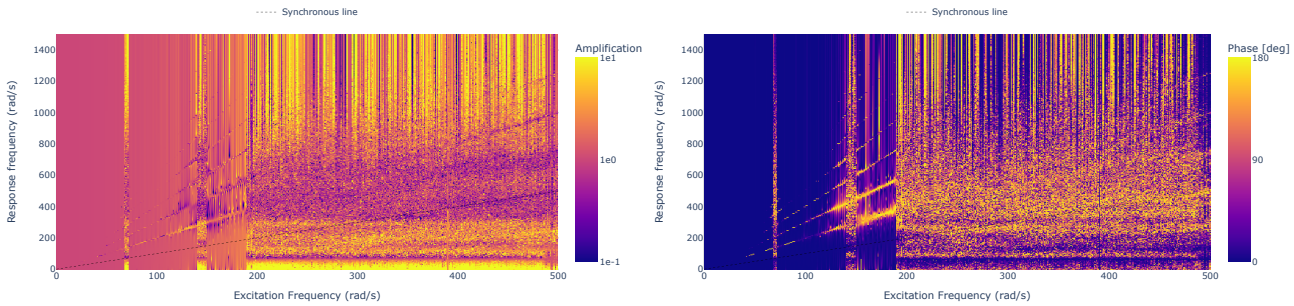

(a) (b)

Figure 8: Spatially averaged amplification (a) and relative phase (b) between base chain and resonators for excitation amplitude of 9000 N.

structure are responsible for the vibration attenuation. For the non-periodic response, however, something entirely different takes place, with seemingly randomised relative phase and broad spread of the frequency content.

CONCLUSIONS

This work presented the concept of vibration attenuation behavior on nonlinear metamaterials. The results show that the arrangement of graded bi-stable resonators can produce broadband vibration attenuation for a simple 1-D periodic lattice system. The attenuation band and mechanisms involved are strongly dependent on the excitation amplitude due to the occurrence of chaotic behavior.

The results showed that clearly distinct mechanisms were at play during periodic and chaotic responses. Periodic multiharmonic behavior exhibits similar characteristic as those observed on linear locally resonant systems, in which the

amplitude and phase relationships between resonators and base structure are responsible for the attenuation effects.

After the onset of chaos, however, the phase and amplitude relations become apparently randomized, with no consistent pattern that would explain the attenuation observed as it does for the linear case. On the other hand, the spatial distribution of vibration energy revealed that during chaotic behavior the energy transferred to the resonators are significantly increased, which reflects a reduction of its effective mechanical impedance and consequently an increase in the base structure‘s impedance.

ACKNOWLEDGMENTS

The authors are grateful to the Brazilian National Council of Research (CNPq - Brazil), processes number 310850/2019-3, 433730/2018-8, 420304/2018-5 and 314168/2020-6, the São Paulo Research Foundation (FAPESP - Brazil), project number 2018/15894-0 and the Federal District Foundation for Research Support (FAPDF -Brazil), project number 00193-00000766/2021-71 for the support.

REFERENCES

[1] M. I. Hussein, M. J. Leamy, M. Ruzzene, Dynamics of phononic materials and structures: Historical origins, recent progress, and future outlook, Applied Mechanics Reviews 66 (4) (2014) –. doi:10.1115/1.4026911.

[2] T. Vasileiadis, J. Varghese, V. Babacic, J. Gomis-Bresco, D. Navarro Urrios, B. Graczykowski, Progress and perspectives on phononic crystals, Journal of Applied Physics 129 (16) (2021) 160901. doi:10.1063/5.0042337.

[3] S. Dalela, P. S. Balaji, D. P. Jena, A review on application of mechanical metamaterials for vibration control, Mechanics of Advanced Materials and Structures (2021) 1–26doi:10.1080/15376494.2021.1892244.

[4] L. Wu, Y. Wang, K. Chuang, F. Wu, Q. Wang, W. Lin, H. Jiang, A brief review of dynamic mechanical metamaterials for mechanical energy manipulation, Materials Today 44 (2021) 168–193. doi:10.1016/J.MATTOD.2020.10.006.

[5] Y. Xia, M. Ruzzene, A. Erturk, Dramatic bandwidth enhancement in nonlinear metastructures via bistable attachments, Applied Physics Letters 114 (9). doi:10.1063/1.5066329.

[6] Y. Xia, M. Ruzzene, A. Erturk, Bistable attachments for wideband nonlinear vibration attenuation in a metamaterial beam, Nonlinear Dynamics 102 (3) (2020) 1285–1296. doi:10.1007/s11071-020-06008-4.

[7] P. Sheng, X. Fang, J. Wen, D. Yu, Vibration properties and optimized design of a nonlinear acoustic metamaterial beam, Journal of Sound and Vibration 492 (2021) 115739. doi:10.1016/j.jsv.2020.115739.

[8] T. Kanamaru, Duffing oscillator, Scholarpedia 3 (3) (2008) 6327, revision #91210. doi:10.4249/scholarpedia.6327.

[9] T. Detroux, L. Renson, L. Masset, G. Kerschen, The harmonic balance method for bifurcation analysis of large-scale nonlinear mechanical systems, Computer Methods in Applied Mechanics and Engineering 296 (2015) 18–38. doi:https://doi.org/10.1016/j.cma.2015.07.017.

[10] K. Lust, Improved numerical floquet multipliers, International Journal of Bifurcation and Chaos 11 (09) (2001) 2389–2410.

[11] E. M. Baily, Steady-state harmonic analysis of nonlinear networks, Stanford University, 1968.

[12] G. Floquet, Sur les équations différentielles linéaires à coefficients périodiques, in: Annales scientifiques de l'École normale supérieure, Vol. 12, 1883, pp. 47–88.

[13] A. L. Skubachevskii, H.-O. Walther, On the floquet multipliers of periodic solutions to non-linear functional differential equations, Journal of Dynamics and Differential Equations 18 (2) (2006) 257–355.

[14] A. A. Brandão, A. S. de Paula, A. T. Fabro, Rainbow gyroscopic disk metastructures for broadband vibration attenuation in rotors, Journal of Sound and Vibration 532 (2022) 116982.

RESPONSIBILITY NOTICE

The authors are the only responsible for the printed material included in this paper.